Supplementary Information

Thermally-Modulated Multilayered Graphene Oxide for Hydrogen Storage

Byung Hoon Kim[ab], *Won G. Hong*[a], *Han Young Yu*[c], *Young-Kyu Han*[a], *Sang Moon Lee*[a], *Sung Jin Chang*[a], *Hoi Ri Moon*[b], *Yongseok Jun*[b], *and Hae Jin Kim*[*a]

[a]Division of Materials Science, Korea Basic Science Institute, Daejeon, 305-333, Republic of Korea

[b]Interdisciplinary School of Green Energy, KIER-UNIST Advanced Center for Energy, UNIST, Ulsan, 689-798, Republic of Korea

[c]Next Generation Energy Technology Team, Electronic and Telecommunications Research Institute, Daejeon, 305-700, Republic of Korea

Sample characterization

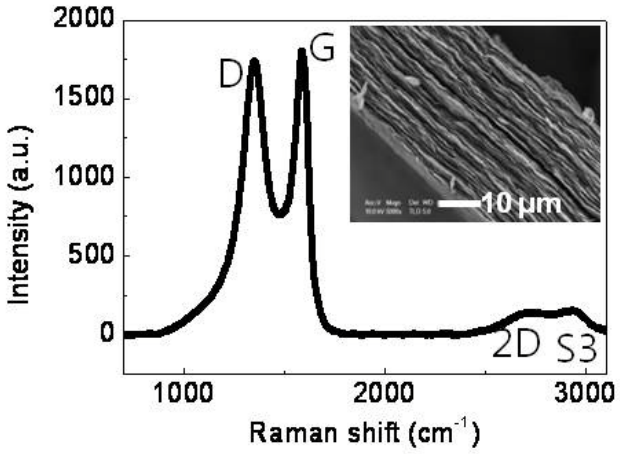

Figure S1. Raman spectroscopy of GO. The inset shows high-resolution SEM side-view images of multilayered GO.

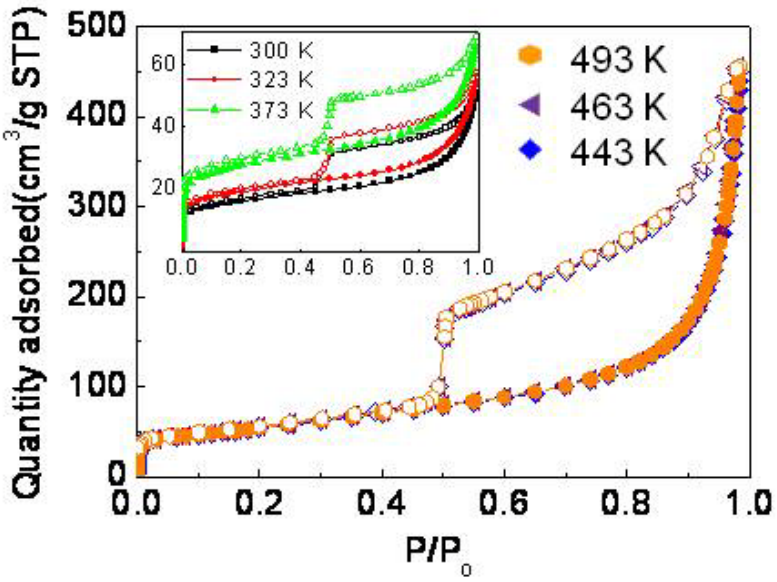

Figure S2. Nitrogen adsorption (solid symbols) and desorption (open symbols) isotherms of thermally modulated GO at 77 K.

NMR study

The representative ^{13}C-MAS (black) and ^{1}H-^{13}C CP MAS (red) NMR spectra for pristine GO are depicted in Fig. S3, which are similar to that of GO in the previous literature[S1]. From the well resolved ^{13}C MAS NMR peaks, one could assign to the carbon site, graphitic sp^2 carbon at 137 ppm, three characteristic functional groups for GO at 171 (O=C–O), 71 (C–OH), and 63 (C–O–C) ppm. ^{13}C CPMAS NMR spectrum of pristine GO exhibits four well-resolved NMR peaks at 133 (graphitic sp^2), 103 (O–C–O), 71 (C–OH), and 62 (C–O–C) ppm. The cross polarization effect increases the relative intensity of the hydroxyl group (71 ppm), largely due to the magnetization transfer from proton to the carbon center. Thus, it appears that the hydroxyl group in pristine GO contains an electron acceptor functionality.

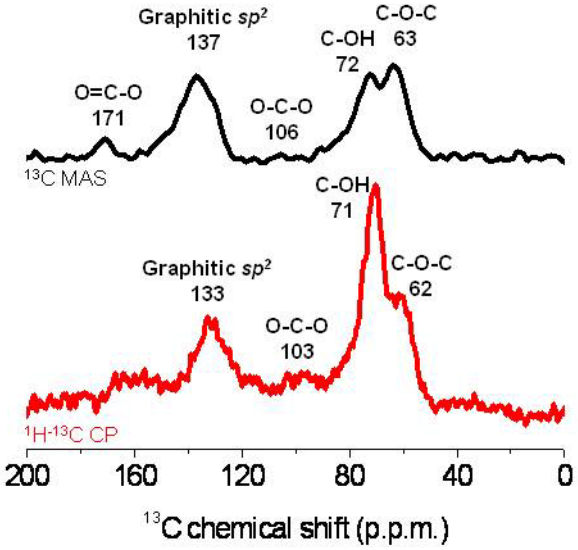

Figure S3. ^{13}C-MAS (black) and ^{1}H-^{13}C CP (red) NMR spectra of pristine multilayered GO.

Micro Raman mapping

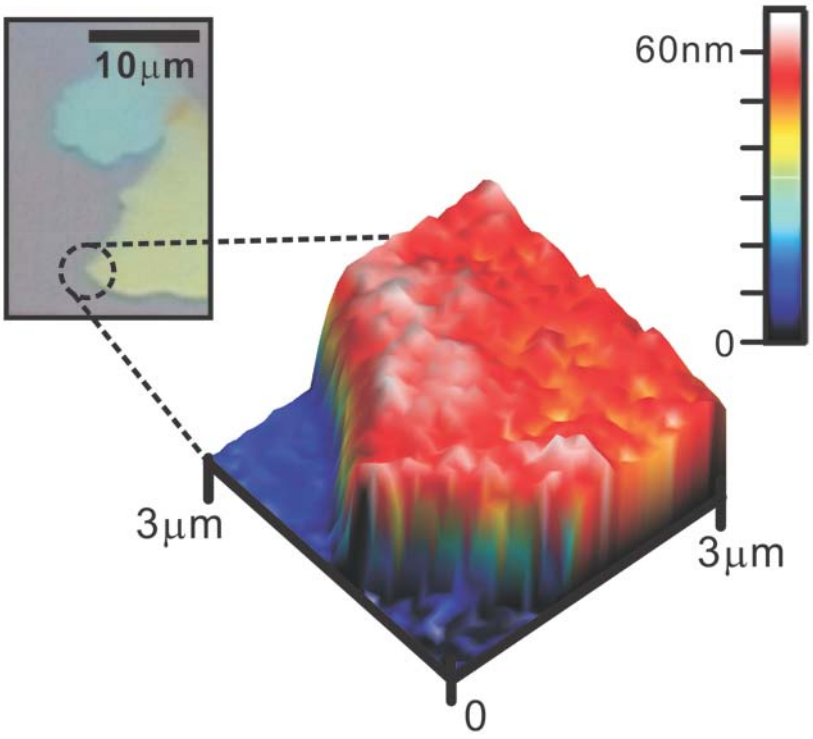

Figure S4. Topography for a part of the multilayered GO with atomic force microscopy (AFM) shows the average height of GO of 60 nm. The image on the left is the optical image of a large GO.

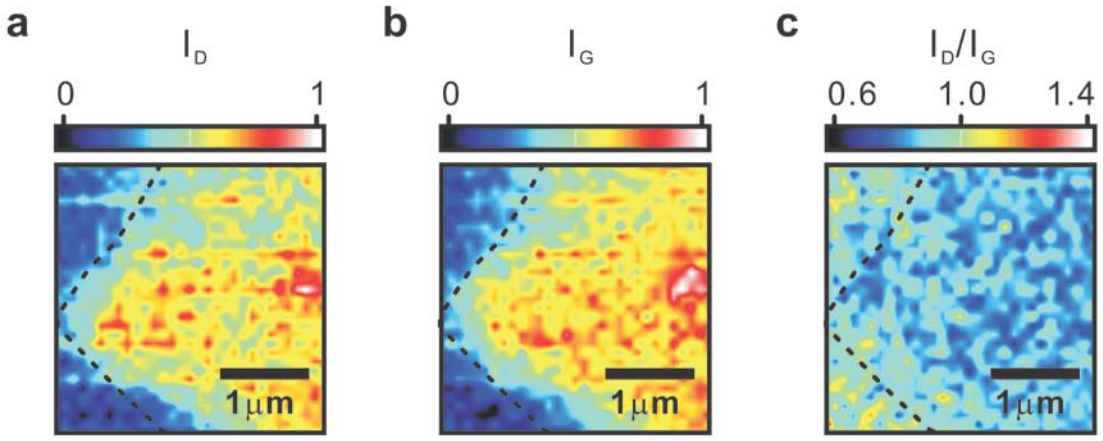

Figure S5. Raman mapping of GO in air. a, b, and **c** are I_D, I_G, and ratio of I_D/I_G, respectively. Spatially resolved Raman spectroscopy for GO in air revealed D and G band signals are mostly distributed in the center of GO.

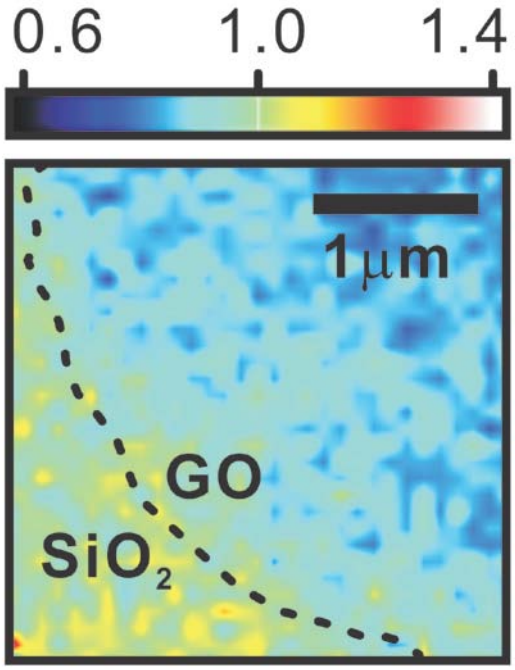

Figure S6. I_D/I_G ratio after the H_2 adsorbed GO was left in air for 3 days. It is similar to that of GO in air, indicating the main adsorption occurs by physisorption.

Table S1. BET surface area and pore volume of GOs. T_a-dependent surface area S (m^2/g) and pore volume V (cm^3/g).

T_a (K)	S (m^2/g)	V (cm^3/g)
300	57.5	0.076
323	69.3	0.084
373	100.8	0.106
443	183.1	0.633
463	186.1	0.675
493	192.1	0.689

Table S2. Variation of interlayer distance and H_2 storage capacity. T_a-dependent interlayer distance x (Å) and H_2 uptake (wt%) values at 9.0 MPa.

	77 K		298 K	
T_a (K)	x (Å)	H_2 uptake	x (Å)	H_2 uptake (wt%)
300	6.705	1.132	7.605	0.2802
323	6.644	1.604	6.685	0.2850
373	6.524	2.684	6.587	0.3563
443	6.467	4.150	6.531	0.4914
463	6.386	4.805	6.414	0.4833
493	6.845	4.352	6.705	0.4622

Data fitting procedure

We fitted the experimental data to a log normal distribution function to obtain the optimal interlayer distance (x_m) and maximum H_2 uptake values from our observed data. The distribution function between the number of absorbed hydrogen molecules (N in g^{-1}) and interlayer distance of GO (x in Å) is

$$N = N_0 + \frac{N_S}{\sqrt{2\pi}\sigma x}\exp\left[-\frac{\left\{\ln\left(x/x_m\right)\right\}^2}{2\sigma^2}\right] ,$$

where N_0 is the number of adsorbed H_2 on a single layer of GO, N_S is the number of H_2 per unit area and unit mass of GO ($Å^{-2}g^{-1}$), and $1/\sigma$ ($Å^3$) is the volume occupied by the same number of H_2 at each pressure.

Table S3. The number of adsorbed H_2 on a single-layer GO (N_0), the volume occupied by the same number of H_2 (σ), and the number of H_2 per unit area and unit mass of GO (N_S) at 298 K.

P (MPa)	N_0 (10^{20} g^{-1})	σ ($Å^{-3}$)	N_S (10^{20} $Å^{-2}g^{-1}$)
6.00	4.405 ± 0.0265	0.0154 ± 0.0003	0.642 ± 0.0088
7.50	7.001 ± 0.7990	0.0182 ± 0.0045	1.657 ± 0.2896
9.00	8.344 ± 0.8403	0.0188 ± 0.0039	2.203 ± 0.3131

References

S1. Gao, W.; Alemany, L. B.; Ci, L.; Ajayan, P. M. New insight into the structure and reduction of graphite oxide. *Nature Chem.*, 2009, **1**, 403-408.